frontiers | Frontiers in Marine Science

ORIGINAL RESEARCH
published: 31 May 2022
doi: 10.3389/fmars.2022.846976

REE Anomalies Changes in Bottom Sediments Applied in the Western Equatorial Atlantic Since the Last Interglacial

*Thiago A. Sousa[1], Igor Martins Venancio[1], Eduardo Duarte Marques[2], Thiago S. Figueiredo[1], Rodrigo Azevedo Nascimento[1], Joseph M. Smoak[3], Ana Luiza S. Albuquerque[1], Claudio Morisson Valeriano[3,4] and Emmanoel Vieira Silva-Filho[1]**

[1] Geoscience (Geochemistry) Graduate Program (Environmental Geochemistry), Fluminense Federal University, Niterói, Brazil, [2] Geological Survey of Brazil (SGB/CPRM), Belo Horizonte Regional Office, Belo Horizonte, Brazil, [3] School of Geosciences, University of South Florida, St. Petersburg, FL, United States, [4] Tektos - Geotectonic Research Group of the Faculty of Geology, State University of Rio de Janeiro (UERJ), Rio de Janeiro, Brazil

OPEN ACCESS

Edited by:
Miguel Angel Huerta-Diaz, Autonomous University of Baja California, Mexico

Reviewed by:
Yuan-Pin Chang, National Sun Yat-sen University, Taiwan
Daniel Smrzka, University of Vienna, Austria

***Correspondence:**
Emmanoel Vieira Silva-Filho
emmanoelvieirasilvafilho@id.uff.br

Specialty section:
This article was submitted to Marine Biogeochemistry, a section of the journal Frontiers in Marine Science

Received: 31 December 2021
Accepted: 19 April 2022
Published: 31 May 2022

Citation:
Sousa TA, Venancio IM, Marques ED, Figueiredo TS, Nascimento RA, Smoak JM, Albuquerque ALS, Valeriano CM and Silva-Filho EV (2022) REE Anomalies Changes in Bottom Sediments Applied in the Western Equatorial Atlantic Since the Last Interglacial. Front. Mar. Sci. 9:846976. doi: 10.3389/fmars.2022.846976

We reconstruct paleoredox conditions in the Western Equatorial Atlantic (WEA) over the glacial-interglacial cycle (~130 ka) by using new high-resolution REEs data and their anomalies from a marine sediment core (GL-1248) collected from the equatorial margin off the continental shelf of NE Brazil. This approach aims to improve the understanding of the dynamics of paleoclimatic and sedimentary inputs on the coast of northeastern Brazil. Marine sediments were analyzed *via* Mass Spectrometry (ICP-MS) after total digestion with HF/HNO_3. REEs proxies are a useful tool in understanding the transport and origin of sediments due to their physicochemical properties. Our data showed the Parnaíba River was the main source of REEs content in the western South Atlantic. Fe minerals (Fe-oxyhydroxides) produced *via* weathering of continental and tropical soils were the principal REE-carrier phase during transportation and ultimate deposition at core site GL-1248. Several regional climatic factors mainly rainfall changes contributed significantly to continental-REEs erosion of sedimentary layers of the Parnaíba Basin, and transport and deposition of the mobilized REEs from the continent to the study site. Furthermore, changes in the negative Ce-anomaly showed low variation along the core indicating a reduction in deep ocean oxygenation during the interglacial relative to the last glacial period. That variation, probably, was associated with glacial-interglacial variations in sea level with the exposure of the continental shelf. The origin of positive Eu anomalies in siliciclastic sediment, also observed in the core, was explained by preferential retention by feldspars such as plagioclases and potassium feldspars mostly from the assimilation of felspar during fractionation crystallization of felsic magma in the Parnaíba basin since the Last Interglacial.

Keywords: Rare Earth Elements, glacial-interglacial, weathering, Parnaíba Basin, sea level, Northeast Brazil

INTRODUCTION

The pattern of abundance in rare earth elements (REEs) has been applied as a reliable geochemical tool in paleoenvironmental and paleoclimatic studies to trace weathering, provenance, and climate changes that have occurred on the continent during the past (Taylor and McLennan, 1985). This is possible due to the physical and chemical characteristics of the REEs due to their electron configuration (+3), poor solubility, and the low concentrations in the waters of rivers and oceans. The REEs utility is further enhanced by its strong binding capability with sediments, low natural background levels, chemical stability, and low mobility (Antonina et al., 2013). Furthermore, REEs has a specific chemical behavior along the sedimentary column and differences in atomic weight strongly allows fractionation during geochemical processes that can be observed *via* normalization (Yusof et al., 2001). The exception to this rule is Ce and Eu, which, unlike the other REEs, can be subjected to the effects of redox processes, alternating their trivalent valences to Ce^{4+} and Eu^{2+} (De Baar et al., 1983; German and Elderfield, 1990).

Over the last few decades, much attention has been given to the application of Ce anomalies in paleoceanographic studies examining bottom water redox conditions (Wright-Clark and Holser, 1981; Elderfield and Pagett, 1986; Wang et al., 1986; Liu et al., 1988; Liu and Schmitt, 1990; Pattan et al., 2005; Tostevin et al., 2016), tectonic and stratigraphic reconstruction (Murray et al., 1990a; Murray et al., 1990b), diagenetic process (German and Elderfield, 1990; Murray et al., 1991) and as a potential indicator of eustatic sea-level changes (Wilde et al., 1996). Moreover, Ce-anomalies may help identify systematic variations in the sedimentary column, and the evolution of the environment by natural processes of continental erosion and autochthonous supply by continental shelf environments (Tostevin et al., 2016). Thus, it is also possible to investigate past climatic events and their consequences for the sedimentary dynamics (Xu et al., 2011). However, studies focusing on using REEs proxies for understanding paleoredox conditions in the western equatorial Atlantic (WEA) are still scarce. A wide approach on the topic is limited by the fact that in tropical/equatorial regions, the chemical and mineralogical composition of the sediment transported by rivers is strongly dependent on parent rock in the drainage basin, the intensity of weathering, and various grain sizes effects (Bouchez et al., 2011; Rousseau et al., 2019).

A recent study by Bohm et al. (2015) indicated a strong rate of ventilation in the deep Atlantic during interglacial periods. In the middle to deep Atlantic, a higher oxygenation rate was observed during the same period concerning glacial periods (Jaccard and Galbraith, 2012; Hoogakker et al., 2015). Moreover, millennial variations in redox conditions in the deep Atlantic are widely observed during the last glacial period (Hoogakker et al., 2015; Gottschalk et al., 2016). The reduction in glacial ocean oxygenation was possibly caused by increases in the biological pump, due to the remineralization of organic matter, and by the decrease in the rate of deep ocean ventilation associated with the reorganization of ocean circulation. Meanwhile, the Atlantic meridional overturning circulation (AMOC) in its warm mode during interglacial periods ventilates the mid-to-deep Atlantic Ocean (Rahmstorf, 2002). Many studies support the accumulation of remineralized carbon in the deep ocean during glacial periods (Curry and Oppo, 2005; Chalk et al., 2019). Given the depth of the GL-1248 sediment core (2264 m), it is expected to record changes in mid-depth Atlantic redox conditions over the last glacial-interglacial variation cycle.

Here, we present high-resolution data for the reconstruction of paleoredox conditions in the WEA over the glacial-interglacial cycle using REEs content and their anomalies from marine sediment core (GL-1248) collected along the equatorial Brazil margin off the continental shelf of NE Brazil. In addition, we compare our data with other relevant geochemical proxies and mineralogical information, to better constrain the causes behind the observed paleoredox changes, related to both drivers on the continent and Brazilian equatorial margin.

MATERIALS AND METHODS

Location, Lithology, and Sampling

A 19.29-m long marine sediment core (GL-1248) was collected at a water depth of 2264-m by Petróleo Brasileiro S.A. (Petrobrás) on the continental slope off the coast of northeastern Brazil (0°55.2'S; 43°24.1'W). The core location was 170 km off the coastline and 280 km to the north of the mouth of the Parnaiba River (**Figure 1**).

Venancio et al. (2018) previously described the lithological composition of GL-1248. It consists of greenish to olive sediments rich in silty clay between 1.00-12.99 m and 16.60-19.29 m. The sedimentary interval between 0-1.00 m and 12.99 to 16.60 m contains carbonate-rich sediments represented by more reddish and whitish clays.

The sub-sampling from core GL-1248 was conducted at the Operational Oceanography Laboratory (LOOP- UFF) by slicing at a resolution of 1 sample for every 4 centimeters. These samples were identified with core ID (GL-1248) followed by layer number, packed in an ultra-freezer, and subsequently freeze-dried. The lyophilized samples were ground using an agate mortar to homogenize particle size. The dry powder was weighed on a high precision analytical balance with 150 mg per sample and posteriorly inserted into porcelain crucibles. After that, the vessel was left in a muffle oven heated to 500°C for about 4 hours to eliminate the organic matter.

Sediment Core Chronology

The depth-age model of GL-1248 indicated the core covers the last 130 thousand years (details of the depth-age model can be seen at Venancio et al., 2018). The age model is based on 12 Accelerator Mass Spectrometry (AMS) radiocarbon ages for the upper 6.30-m core depth (~ 43.670 ka). For the lower part of core GL-1248 (6.30 to 16.66 m core depth; ~ 44-128 ka), ages were obtained through the alignment of the Ti/Ca ratio to the ice $\delta^{18}O$ record of the North Greenland Ice Core Project (Members, 2004; Wolff et al., 2010). They were established as MIS 1 (starts at 14 ka before present), MIS 3 (29–57 ka), MIS 4 (57–71 ka), MIS 5a (peak at 82 ka), MIS 5b (peak at 87 ka), MIS 5c (peak at 96 ka), MIS 5d (peak at 109 ka), MIS 5e (peak at 123 ka).

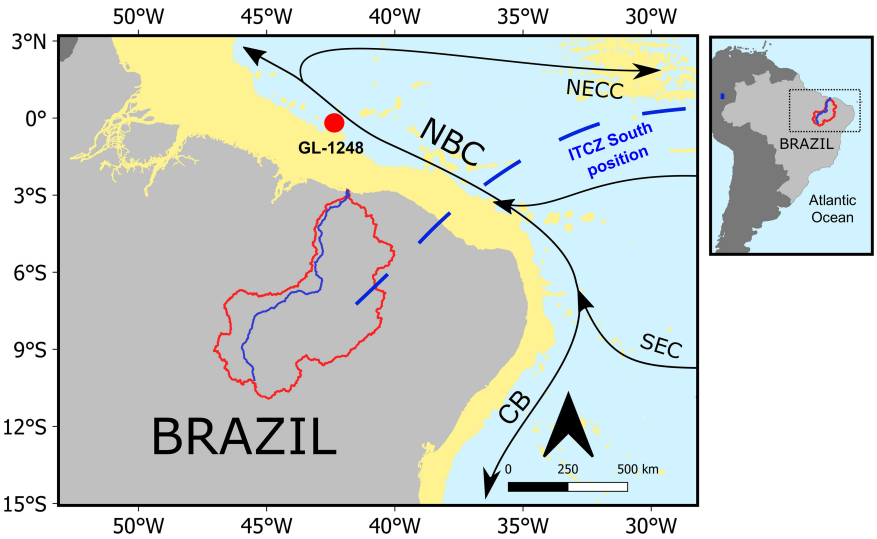

FIGURE 1 | The regional map shows the location of marine core GL-1248 from the western equatorial Atlantic (WEA) with the southmost position of the Intertropical Convergence Zone (ITCZ) during the end of austral summer (March-April). The core is represented by the red dot in geographic coordinates 0°55.2'S, 43°24.1'W; 2.264 m. The map also shows relevant surface currents such as the South Equatorial Current (SEC), North Equatorial Countercurrent (NECC), Brazilian Current (BC), and the North Brazil Current (NBC) in black arrows. The dashed blue line displays the approximate southern position of the Intertropical Convergence Zone (ITCZ) during austral summer (December–March). Source: References of Paleorecords according to Wang et al. (2004); Nace et al. (2014), Dupont et al. (2010), Zhang et al. (2015), figure adapted by Piacsek, 2020.

Geochemical Analysis

As described by Fadina et al. (2019), core GL-1248 was sampled every 4 cm (323 total samples) for bulk analyses, as Total Organic Carbon (TOC, in %) and stable isotopes ($\delta^{13}C$ and $\delta^{15}N$) analyses. Each sample was encapsulated in a tin (Sn) capsule after carbonate removal *via* acidification with 1 M HCl, 60 mg of dried and pulverized sediment. The bulk analysis was performed using a PDZ Europa ANCA-GSL elemental analyzer at the Stable Isotope Facility of the University of California, Davis (USA) with an analytical precision of ± 0.09%.

Elemental intensities of core GL-1248 (Fe, Ti, Ca, K, Al, and Mn) were obtained by scanning the split core surfaces of the archive halves with X-ray fluorescence Core Scanner II (AVAATECH Serial number 2), which is a semi-quantitative method for stepwise geochemical characterization of sediment cores at MARUM, University of Bremen (Germany). The XRF measurements were made downcore every 0.5 cm by irradiating 10 mm to 12 mm of the surface for the 20s at 10 kV. For a detailed description of the method, see Venancio et al. (2018).

REE Preparation

The approximately 0.150 g of the marine sediments samples (a total of 310) were roasted in muffle furnace for 2 hours at 450°C. After roasting time was achieved, samples were unloaded immediately from muffle furnace and were kept in desiccator to cool down. Each roasted samples were reweighed on a high precision analytical balance (± 0.0001g precision) to a total weight of about 0.1 g and added in the vessel to be digested in a Microwave (Speedwave®four - Berghof) with 4.0 mL mono-distilled nitric acid (HNO_3 65%) and 1.0 mL hydrofluoric acid (HF 70%) using the established US EPA method (Environmental Protection Agency 3052 Method). The goal of this method is total samples decomposition with judicious choice of acid combinations to give the highest recoveries for the target analytes. The mono-distilled nitric acid (HNO_3 65%) was used to effect sample digestion in microwave, while hydrofluoric acid (HF 70%) is capable of dissolving silicates contained in the sample. At the end of the process, the resulting solution was filtered with chemical analysis qualitative filter paper into a second acid-cleaned container and added the volume up to 15 mL with dilute solutions of boric acid (H_3BO_3) to avoid problems with HF permitting the complexation of fluoride to protect the quartz plasma torch. REEs and some trace elements (U and Th) of core GL-1248 were measured by ICP-MS (NexION 300D, Perkin Elmer, USA) at the LEA (Atomic Spectrometry Laboratory) at the Federal University of Espirito Santo (UFES). De Sousa et al. (2021) described the analytical standard procedures in detail. REEs patterns for selected samples from the core were normalized according to Post-Archean Australian Shale (PAAS) (Taylor and McLennan, 1985; Pourmand et al., 2012). The analytical precision and accuracy were better than ± 8% for the investigated elements. This was assessed with reference material (PACS-2 - Marine Sediment Reference Materials for Trace Metals and other Constituents) and by the results of the duplicate measurements of eight sediment samples, as well as duplicate measurements of reference material samples. Rare earth elements were divided into light REEs (LREEs, from La to Nd), middle REEs (MREEs, from Sm to Ho), and heavy

REEs (HREEs, from Er to Lu) according to Henderson (1984) and their ratios were calculated.

Cerium Anomaly

The extent of the Cerium anomaly is defined by the δCe [Ce]/[Ce*] ratio, where [Ce] is the cerium concentration and [Ce*] is the theoretical non-anomalous value interpolated from La and Nd values, according to the following equation below:

$$Ce/Ce* = 3Ce_N/(2La_N + Nd_N) \quad \text{Equation 1}$$

Where "**N**" refers to REEs normalized by Post Archean Average Australian Shale (PAAS; (Taylor and McLennan, 1985).

When Ce is relatively depleted compared to other REEs (Ce/Ce* < 1) a negative Ce-anomaly is observed suggesting an oxic environment condition (German and Elderfield, 1990; Pattan et al., 2005). Conversely, a positive Ce-anomaly results when Ce is enriched relative to its neighbors (Ce/Ce* > 1), suggesting anoxic/suboxic environment condition (German and Elderfield, 1990; Pattan et al., 2005).

Europium Anomaly

Another similar REEs anomaly that is occasionally recorded by Europium, represented by the δEu [Eu/Eu*] ratio, where [Eu] is the europium concentration and [Eu*] is the value obtained at the europium position by straight-line interpolation between the plotted points for Sm and Gd, according to the following equation below:

$$Eu/Eu* = Eu_N/(Sm_N + Gd_N)^{1/2} \quad \text{Equation 2}$$

where N refers to PAAS-normalized values developed by Pourmand et al. (2012).

Where "**N**" refers to REEs normalized by Post Archean Average Australian Shale (PAAS; (Taylor and McLennan, 1985).

When Eu is relatively enriched compared to other REEs (Eu/Eu* > 1) a positive Eu-anomaly suggests sediments and some sedimentary rocks containing a high amount of feldspar minerals, while negative Eu-anomaly indicate depletion or fractionation of the same mineral (Absar and Sreenivas, 2015; Liu et al., 2015).

Mineralogical Analysis

Mineralogical characterization was performed on 40 pulverized representative samples distributed within each marine oxygen isotope stage (MIS) of core GL-1248, using an X´PERT PRO MPD (PW 3040/60) X-ray powder diffractometer (XRD) with CuKα1 radiation (λ = 1,5406 Å) at the Mineral Analysis Laboratory (LAMIN), Mineral Resources Research Company (CPRM), Manaus, Amazonas, Brazil. Diffractograms were collected using Voltage 40kv, Current 40A, 2⊖ between 5° to 70° with a step size of 0.02° and 50s scanning time. For mineral identification, generated patterns were compared with a database from the International Center for *Diffraction Data – Powder Diffraction File* (ICDD-PDF). The patterns are specific to each mineral (i.e. quartz, 46-1045), and there may be different patterns for the same mineral, especially when there are variations in the chemical composition, solid solutions, etc.

RESULTS

Age Model and Sedimentation Rates

The depth-age model of core GL-1248 based on the AMS radiocarbon ages for the upper 6.3-m depth yielded an age of 44.0 ± 0.7 ka. For the lower part of the core (6.30 to 16.66 m core depth) ages were obtained through the alignment of the Ti/Ca ratio and the $\delta^{18}O$ record from the North Greenland Ice Core Project (Members, 2004; Wolff et al., 2010) with ages ranging from 44.0-129.0 ka. The sedimentary record includes a sedimentary hiatus between 2.18 m and 1.70 m (29.1 and 14.8 ka, respectively).

The sedimentary core profile comprises 4 marine isotope stages (MIS 1 to 5, excluding 2) according to changes in temperature derived from deep-sea core sample data (Lisiecki and Raymo, 2005). Diverse sedimentation rates (SR) are observed over MIS indicating a large fluctuation within the record (**Figure 2**). During MIS 5 (from ~ 128.0 ka to 71.0 ka), SR varies with the highest occurring within the MIS 5a (25.7 cm/kyr), whereas rates during MIS 5e are relatively constant at 6.93 cm/kyr. The glacial period MIS 4 (from ~ 71.0 ka to 57.0 ka) started with low SR (an average value of 13.0 cm/kyr) and increased notably during MIS 3 (from ~ 57.0 ka to 29.0 ka) reaching an average value of 32.1 cm/kyr.

An unusually low SR (3 cm/kyr) between 2.18 and 1.70-m core depth (from ~ 14.0 and 29.0 ka) is due to the hiatus, as reported for the region and period, although no significant lithological changes were observed. The hiatus covers every Henrich Stadials 1 (HS 1), where is characterized by abrupt records, on a millennial-scale, of precipitation in northeastern Brazil (Arz et al., 1998; Cruz et al., 2006; Zhang et al., 2015). This increase in the frequency of rainfall intensity also occurred within the Parnaíba River Basin and increased the discharge of terrestrial material to the ocean. Continuously, the entry of more continental debris favored greater kinetic and drag energy to the mouth of the Parnaíba River and the steep continental slope. The core GL-1248 was collected in a region with a high slope and under the influence of these phenomena on a millennial-scale. The origin of the hiatus comes from the high-energy input of the detrital material and the steep angle of the continental slope, which caused a collapse in the sedimentary record during sedimentation. Finally, the SR values during MIS 1 (starts at 14 ka before present) are irregular. Variations between 5.42 and 24.23 cm/kyr, with the highest values, reached within the interval of occurrence of abrupt events on a millennial-scale recorded (i.e. Younger Dryas) in the intervals 1.26 and 0.69 cm in the depth of core GL-1248.

Total REE and Trace Elements Distribution

The REE concentration vertical distributions of core GL-1248 are plotted in (**Figure 2**). The total REE concentrations (sum of La to Yb, excluding Tb, Ho, Tm, and Lu) of the sediment samples varied between 42.93 and 231.06 μg/g (with an average value of 152.44 μg/g). The highest ΣREE concentration values (231.06 μg/g) were recorded at 78 ka (1258-cm depth) within MIS 5. ΣREE concentrations were particularly high in glacial phases (MIS 4 and MIS 3), as well as in MIS 5a (MIS 5 interglacial sub-stage). In

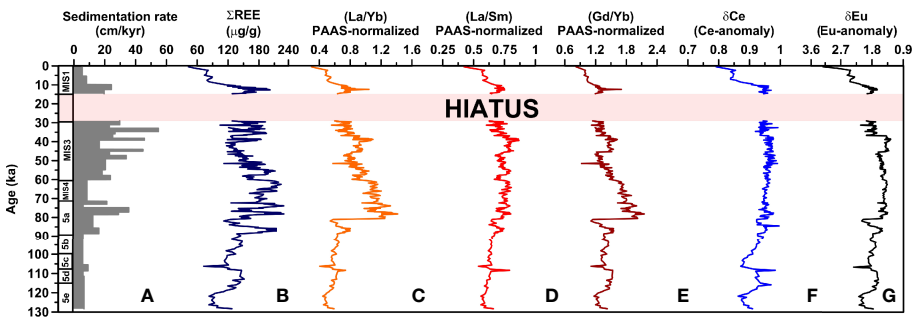

FIGURE 2 | Core GL-1248 profiles of **(A)** Sedimentation rate (cm/kyr) (Venancio et al., 2018), **(B)** ΣREE (μg/g), **(C)** $(La/Yb)_N$, **(D)** $(La/Sm)_N$, **(E)** $(Gd/Yb)_N$, **(F)** δCe (Ce-anomaly), and **(G)** δEu (Eu-anomaly). The dashed light red line marks a hiatus between 14.7 and 29.1 ka. **"N"** is representing the chondrite-normalization by PAAS (Post Archean Australian Shale) (Taylor and McLennan, 1985). Marine isotope stages (MIS) boundaries in this studied time interval are numbered from 1 to 5 (MIS 1, 3, and 5).

comparison, the lowest ΣREE concentration values (42.93 and 55.84 μg/g) were recorded on top-core (0.49 and 1.22 ka, respectively) within the MIS 1. ΣLREE (sum from La to Nd) varied between 30.12 and 198.92 μg/g (with an average of 127.00 μg/g), while ΣMREE and ΣHREE varied between 9.08 and 28.37 μg/g (with an average of 19.57 μg/g), and between 3.73 and 8.46 μg/g (with an average of 5.86 μg/g), respectively. Hence, ΣLREE is more abundant in nature than ΣMREE and ΣHREE. Both the ΣLREE/HREE ratios (8.08-21.84) and the ΣLREE/MREE ratios (3.32-7.97) are lower values than PAAS (28.31 and 10.05, respectively) (**Table S1**) (Taylor and McLennan, 1985). $(La/Yb)_N$ ratios PAAS-normalized varied between 0.30 and 1.42 μg/g (with average of 0.82 μg/g). The $(La/Gd)_N$ and $(Gd/Yb)_N$ PAAS-normalized ratios varied between 0.37 and 0.68 μg/g (with an average of 0.57 μg/g), and between 0.82 and 2.15 μg/g (with an average of 1.43 μg/g), respectively. The REEs profile distributions for their normalized ratios [$(La/Yb)_N$, $(La/Sm)_N$, and $(Gd/Yb)_N$] show a similar value with a marked increase of about 80 ka and a strong decrease of about 14 ka in core GL-1248. This maximum value obtained for REEs profile distribution coincides with the highest SR occurring within MIS 5a (25.7 cm/kyr), as well as a strong decrease in the SR right after abrupt Younger Dryas events (from 16.28 cm/kyr to 8.13 cm/kyr).

Anomalies in δCe and δEu

The negative δCe (Ce/Ce* < 1) values varied from 0.79 to 0.99 (with a mean value of 0.94) over the last 128 ka with a clear abrupt drop from the glacial period (near to 13 ka) to the top core (Interglacial period) (**Table S2**). The highest negative δCe of 0.99 occurs at the bottom core (near to 84 ka; 1341-cm depth), while the lowest negative δCe of 0.79 occur in modern conditions over the interglacial period (0.49 ka near to the top of core). The Interglacial periods (MIS 1 and MIS 5e), and the warm sub-stage of MIS 5 (MIS 5c) with opposing climatic conditions show a relatively large variability with minimum values of 0.79 (top core), 0.86 (~106 ka), 0.871 (~122 ka), respectively. The negative δCe during MIS 4 and MIS 3 has a relatively low variability with mean values ranging between 0.95 and 0.96, respectively.

The positive δEu (Eu/Eu* > 1) values varied from 1.28 to 3.22 (with a mean value of 1.68) with a strong decrease from the top core towards glacial periods (**Table S2**). Hence, the highest positive δEu of 3.22 occurs in the bottom core (near the top core of 0.49 ka), while the lowest positive δEu of 1.28 occurs proximate in the glacial condition around 38.59 ka (523-cm depth). Both modern condition and bottom core with interglacial period show variability with mean values ranging between 2.09 and 1.71, respectively, followed by MIS 3 mean values of 1.59. The highest δEu values coincide with the increase in RSL (relative sea level), and vice-versa (**Figure 2**).

Mineralogy

The mineralogical spectrum obtained through XRD of core GL-1248 revealed a moderate range array of minerals assembly over the last 130 ka. Forty samples were identified in the marine sediment predominantly quartz, calcite, and kaolinite. Other secondary minerals include biotite, feldspars potassium, smectite, calcite magnesium, and halite. The occurrence of iron oxide minerals as goethite was described by Fadina et al. (2019) of core GL-1248. In general, continent-sourced minerals such as quartz and kaolinite were observed during the interglacial and glacial periods (both cold and warm substages). Marine sourced minerals such as calcite were observed also over the core. Smectite clay mineral was identified in small proportions during MIS 4 and MIS 5. (See more in **Table S3**).

DISCUSSION

Glacial-Interglacial Controls on REE-Carrier Phases

Along with geochemical processes, the terrigenous material is transferred to the oceans as suspended sediments in rivers (Milliman and Maede et al., 1983) carrying information about the characteristics of the source areas and past climate changes over the continent (Bentahila et al., 2008; Revel et al., 2010; Revel et al., 2014; Revel et al., 2015; Walter et al., 2000). Weathering,

erosion, transport, deposition, and burial processes control the final composition of the deep-sea sediments (Johnsson et al., 1991; Johnsson, 1993; Morton and Hallsworth, 1999). The geological substrate under the action of weathering and climatic agents reflects a signature characteristic of the adjacent continent to the drainage basins (Depetris et al., 2003). Marine sediment cores have a high capacity to preserve valuable information about changes in sedimentary provenance and continental climate changes (De Sousa et al., 2021). Specifically, REEs are useful, as they do not fractionate during sedimentary processes, which widely distributed in continental rocks. As shown in **Figure 2**, high ΣREE records during glacial periods are coincident with elevated terrigenous depositions recorded in core GL-1248 (Venancio et al., 2018) linked to low relative sea level (Waelbroeck et al., 2002) during glacial periods and millennial-scale changes recorded in Ti/Ca ratios from sediment cores in the WEA (Arz et al., 1998; Wang et al., 2004; Jaeschke et al., 2007; Govin et al., 2012; Nace et al., 2014). These terrigenous loads are characteristic of glacial periods linked to low relative sea levels (Arz et al., 1999; Jaeschke et al., 2007). A combination of regional climatic factors, such as amplified wet deposition with enhanced precipitation and erosion, might be responsible for an increase of REEsconcentration reported in core GL-1248. Overall, REE concentration reported in core GL-1248 mixed in response to glacial-interglacial changes by, providing a high material transport combined with a low sea level. In opposite climatic conditions to glacial periods, as MIS 1 and 5e, beyond the warm sub-stage, MIS 5c exhibited less REE concentration and high sea-level recorded in core GL-1248, because of low regional precipitation and erosion, featuring the warm periods. Hence, REEs peaks that occurred at the end of MIS 5a (230.88 μg/g; ~74 ka) are incompatible with these trends observed in our data over interglacial periods. However, these peaks are coincident with Ti/Ca and Ti/Ca peaks and may be linked to Dansgaard-Oeschger (DO) stadials (**Figure 2**). In opposite, the average REE concentrations were appreciably low over both MIS 1 (125.78 μg/g) and 5e (109.15 μg/g) interglacial periods, when the RSL reached –17.46 m and –13.85 m, respectively. According to Rama-Corredor et al. (2015), over the MIS 5e (SST = 28.9°C) interglacial experienced higher temperatures than MIS 1 (SST = 28.3°C), which are attributed to processional modulation (Martrat et al., 2014). Higher SST observed in interglacial periods are reported in numerous studies as ice sheet reduction and consequently sea level increased by up to 5 m more than modern sea level (Hodgson et al., 2006; Rohling et al., 2007). The increase in sea level has most likely repositioned the mouth of the Parnaiba River farther from the core, reducing the supply of continental material. Therefore, the lower REEs average concentrations displayed in MIS 5e concerning MIS 1 justify the retention of a supply of continental material in the area site of core GL-1248.

Iron oxyhydroxides have an important role in controlling the REEs profile in core GL-1248 and from the correlation between ΣREE composition and $Fe_{(XRF)}$, there were three potential reservoirs (lithogenic, carbonates, and Fe-Mn oxides). A positive correlation with $Fe_{(XRF)}$ can be explained by tropical soil characteristics in the study region (**Figure 3**). In a recent study using the same core, Fadina et al. (2019) observed the presence of iron oxides (and oxyhydroxides) minerals, such as goethite in all samples. In addition, geochemical analysis in the $\delta^{13}C_{org}$ and $\delta^{15}N_{org}$ variations in GL-1248 support the earlier hypothesis that higher amounts of continent-derived materials were deposited on the continental slope of NE Brazil in the glacial periods as opposed to interglacial periods. Thus, these results are consistent with our XRD mineralogy results which follow the same glacial-interglacial alteration in the origin marine sediment GL-1248. In tropical Fe-rich oxide soils, as occur in northeastern Brazil, Fe-oxyhydroxides are important cementing agents and as such play an important role in the metal adsorption processes in this region (Seaman, 2013). According to Bigham et al. (2002) the tropical soil profile of northeastern Brazil was described as having a notable high content of iron oxides mainly goethite and ferrihydrite; an amorphous Fe-oxyhydroxide precursor of hematite formation (Bigham et al., 2002). Hence, REEs content bearing Fe particles derived from the weathering and erosion from the Parnaíba Basin increased in the supply of magnetic material (i.e. magnetite and/or hematite), that was transported by Parnaíba River until they are immobilized on the continental slope. These correlations coincide with an increase in precipitation on the continent in NE Brazil during the wetter conditions related to MIS 4 (De Sousa et al., 2021). Therefore, our results suggests that Fe-oxides may be a principal REE-carrier phase from a marine sediment core GL-1248.

Origin of the Negative Ce-Anomaly in WEA

Studies suggest that the Ce anomaly can be used as a proxy for oxygenation conditions in paleoceanography (German et al., 1990; Schijf et al., 1994; Tostevin et al., 2016). In this study, we presented a sub-millennial resolution record of Ce anomaly since the Last Interglacial. Given the water depth of the sediment core GL-1248 (2.264 m), we expect to observe changes in redox conditions of the mid-depth Atlantic over the last glacial-interglacial cycle. Indeed, our results show a remarkable glacial-interglacial variation (**Figure 4**). A negative Ce anomaly is observed during warm interglacial periods. Conversely, during the end of MIS 5 and over the glacial period, Ce presents no depletion relative to compared to other REEs (Ce anomaly = ~1). Meanwhile, no outstanding millennial variations in the Ce anomaly were observed through the record.

Curiously, our results indicate a reduction in deep ocean oxygenation during the interglacial relative to the last glacial period. These results contradict the well-known notion of a strong deep Atlantic ventilation rate during warm interglacial periods (Böhm et al., 2014). Indeed, previous studies show a higher mid to deep Atlantic oxygenation during interglacial relative to glacial periods (Jaccard and Galbraith, 2012; Hoogakker et al., 2015). Besides, millennial variations in deep Atlantic oxygenation conditions are widely observed during the last glacial period (Hoogakker et al., 2015; Gottschalk et al., 2016), which, despite the sub-millennial resolution, was not found in our Ce anomaly record. The reduced glacial deep ocean oxygenation was caused by an increase in the biological pump, due to the organic matter remineralization, and the decreasing of deep ocean ventilation rate associated with the reorganization of ocean circulation (Hoogakker et al., 2015;

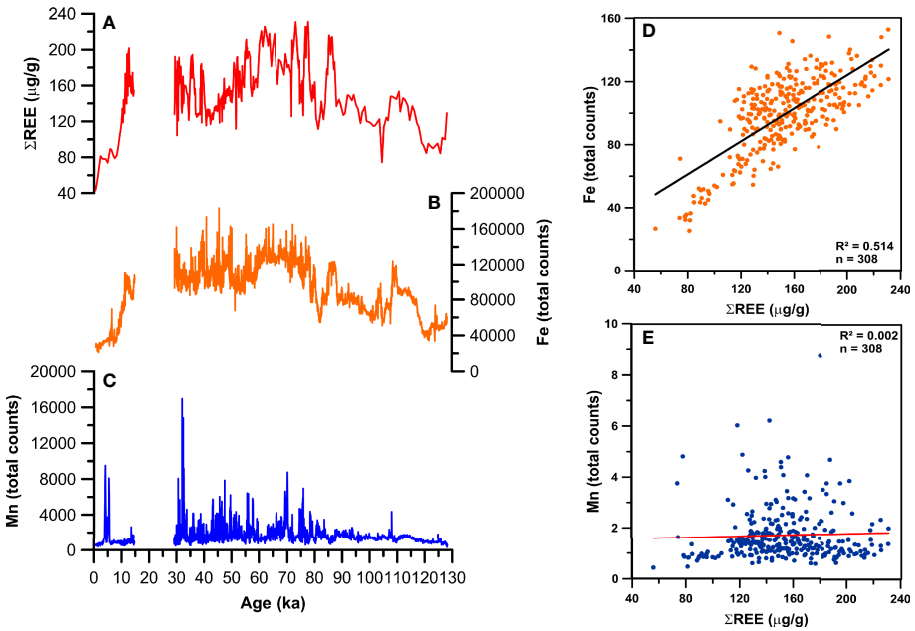

FIGURE 3 | Fe and Mn-REE relationship across the marine sediment studied with; **(A)** Plot of ΣREE concentration (red line) in GL-1248; **(B)** Plot of Fe total counts (orange line) in GL-1248; **(C)** Plot of Mn total counts (dark blue line) in GL-1248; **(D)** positive linear regression between Fe total counts (XRF) and ΣREE indicated by trendline (black line), equation correlation coefficient (R^2 = 0.514); and **(E)** weakly linear regression between Mn total counts (XRF) and ΣREE indicated by trendline (red line), equation correlation coefficient (R^2 = 0.002). ΣREE is shown in µg/g.

Jaccard et al., 2016). Meanwhile, the AMOC in its 'warm' mode during interglacial periods ventilates the mid to deep Atlantic Ocean (Rahmstorf, 2002). Many studies support the accumulation of remineralized carbon in the deep ocean during glacial periods (Curry and Oppo, 2005; Chalk et al., 2019). Together, these results indicate that the Ce anomaly in sediment core GL-1248 was not recording changes in paleoredox conditions of the mid-depth Atlantic in the Brazilian equatorial margin region. This poses the question; what does control the observed glacial-interglacial variation in Ce anomaly? Here we suggest that changes in Ce anomaly were caused by glacial-interglacial variations in sea level through its control on the exposure of the continental shelf. Given its flat morphology, eustatic changes in sea level during glacial-interglacial cycles may result in rapid exposure or drowning of the continental shelf in the Brazilian equatorial margin. Sediment core GL-1248 shows a higher sedimentation rate during the glacial relative to interglacial MIS 5 and MIS 1 (Venancio et al., 2018). This was caused by the lower sea level during glacial periods, allowing terrigenous material, with no Ce anomaly to be discharged directly onto the continental slope, near-site GL-1248. Conversely, during high sea-level periods, the terrigenous input was reduced due to the drowning of the continental shelf, which increased the percentage of biogenic $CaCO_3$ in bulk sediment. Studies indicate that biogenic $CaCO_3$ shows Ce depletion relative to the other REEs, resulting in a negative Ce anomaly in $CaCO_3$-rich sediments (Pattan et al., 2005). Therefore, we argue that a higher proportion of $CaCO_3$ relative to continental material caused the negative Ce anomaly during interglacial periods in GL-1248. Indeed, the reduction in terrigenous input to site GL-1248, as can be exemplified by reduced ΣREE, and enhanced accumulation of biogenic $CaCO_3$ during warm periods in the western equatorial Atlantic (Rühlemann et al., 1996) corroborate our hypothesis.

Given that the continental shelf break starts at about 40 m water depth in the Brazilian equatorial margin, our Ce anomaly only responded to changes in sea level above this isobath. This explains fast changes in Ce anomaly late during termination 1 (~10.5 ka) and no changes during the end of MIS 5 and the over the glacial period when the sea level was near or below the continental shelf break. Furthermore, the similar geochemical behavior of sensitive redox elements such as the Uranium element along the curve of cerium anomalies reinforces the argument that what modulates the conditions discussed within the sediment is not the presence of oxygen in the water column, but the depth of oxygen penetration (**Figure 5**). Additionally, the sedimentation rate can play a key role as they allow more time for the diffusion of uranyl ions from the water column into the sediment (Crusius and Thomson, 2000; Tribovillard et al., 2006).

The Continental Response of Europium Anomalies to Paleoclimate Changes in NE Brazil

Several studies in marine sediments suggest that the positive Eu anomaly is inherited from the content of feldspar in the source bedrock. This is possible due to the easy incorporation of Eu in the structure of felspar during the petrogenetic process. Hence, Eu content in the marine sediments is higher than other REEs

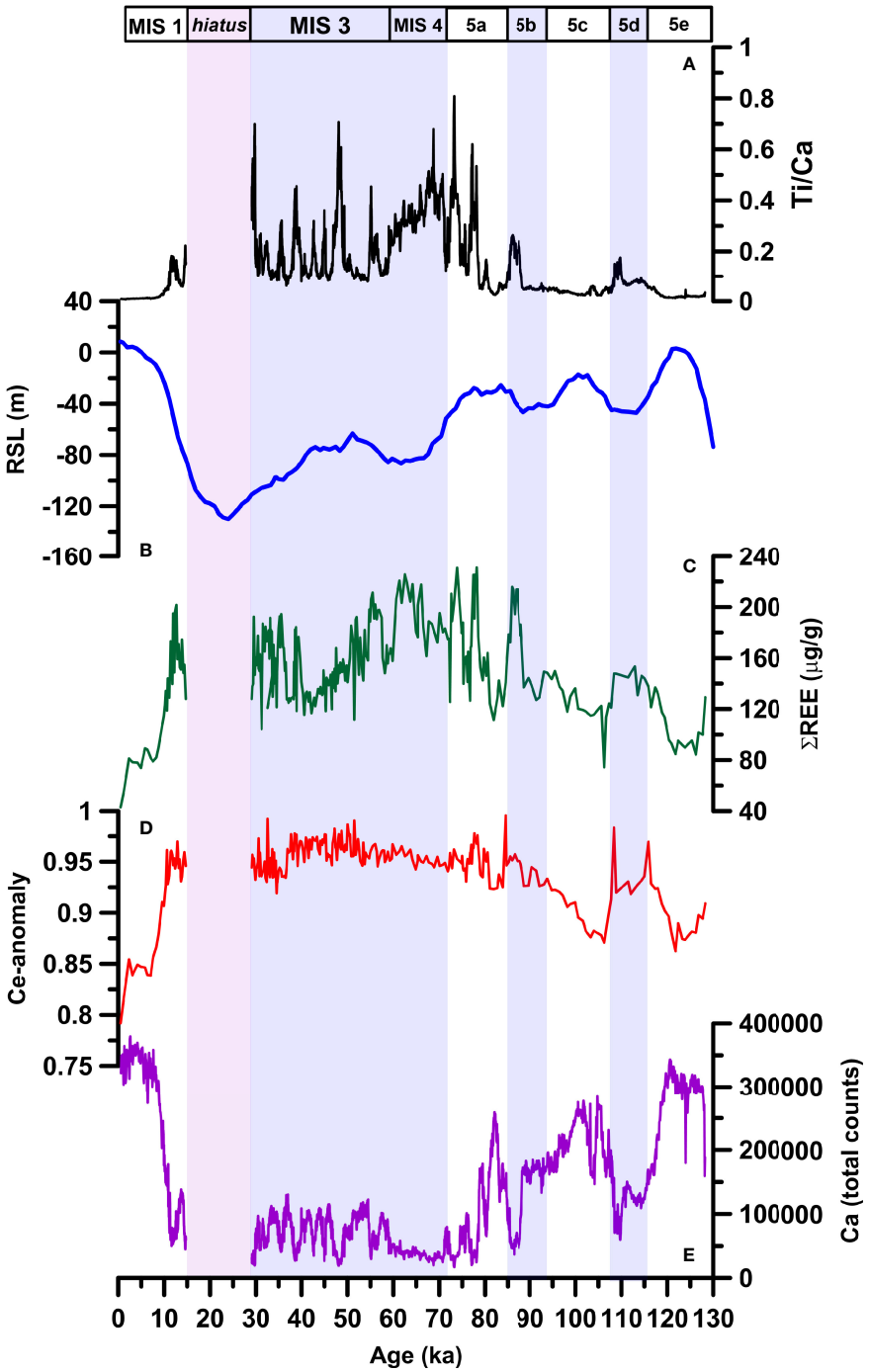

FIGURE 4 | Glacial-Interglacial variability as shown by the comparison between periods of high and low terrigenous sediment delivery to the study site with: **(A)** Ti/Ca ratio from GL-1248 (Venancio et al., 2018) (black line); **(B)** Relative sea level (m) from GL-1248 (Waelbroeck et al., 2002) (dark blue line); **(C)** ∑REE concentration (this study) from GL-1248 (dark green line); **(D)** Ce-anomaly (this study) from GL-1248 (red line); and **(E)** Ca total counts (XRF). MIS boundaries in the studied time interval are numbered from 1 to 5, as well as in the cold substages of MIS 5 (5d and 5b). These cold periods are highlighted in blue bars.

breaking the straight-line shape of the REEs pattern curve (Henderson, 1984; Liu et al., 2015). Positive Eu anomalies and abundances of REEs were reported in sediments and some sedimentary rocks containing feldspar, whereas Eu-depleted felsic igneous rocks and high LREE/HREE ratios, and most basalt does not present Eu anomalies and low LREE/HREE ratios (Absar and Sreenivas, 2015; Liu et al., 2015). The distribution of positive Eu anomaly values observed of core

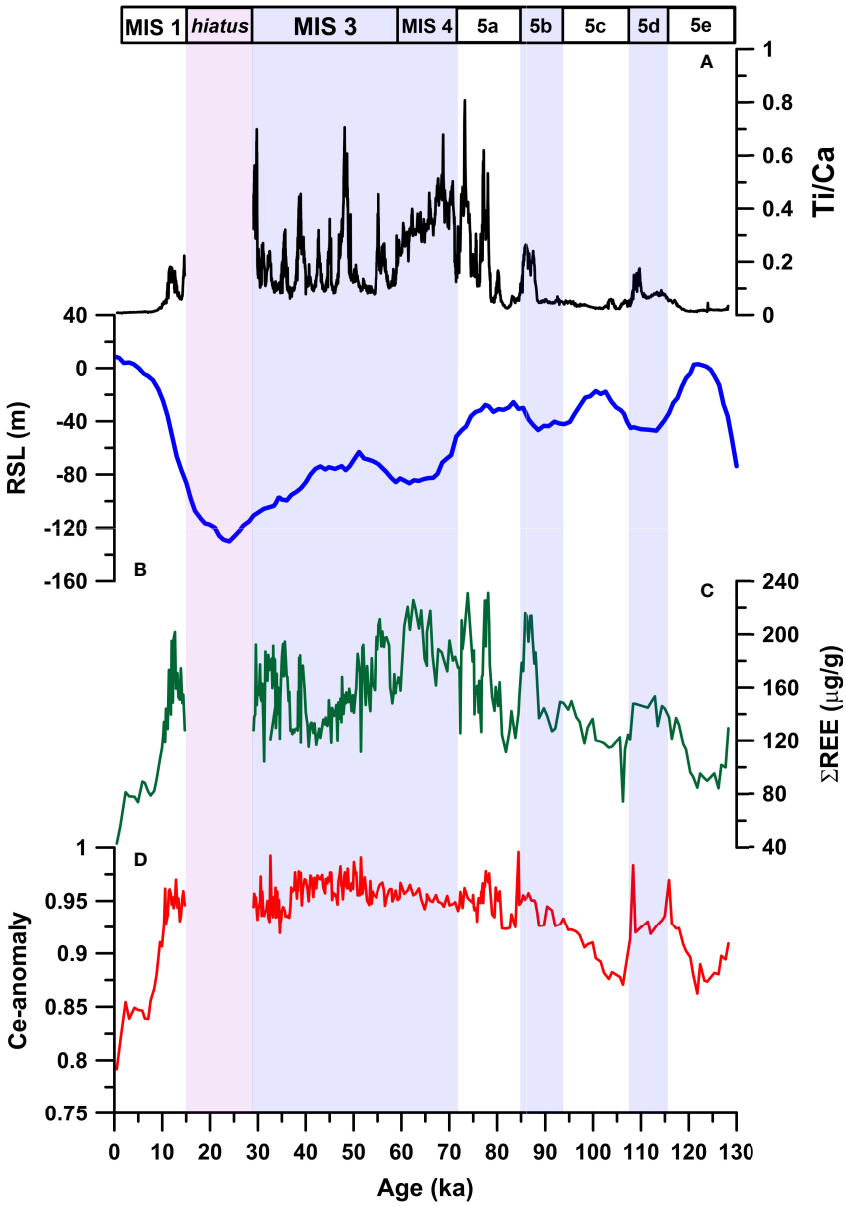

FIGURE 5 | Glacial-Interglacial variability as shown by the comparison between periods of high and low terrigenous sediment delivery to the study site with: **(A)** Ti/Ca ratio from GL-1248 (Venancio et al., 2018) (black line); **(B)** Relative sea level (m) from GL-1248 (Waelbroeck et al., 2002) (dark blue line); **(C)** ΣREE concentration (this study) from GL-1248 (dark green line); and **(D)** Ce-anomaly (this study) from GL-1248 (red line). MIS boundaries in the studied time interval are numbered from 1 to 5, as well as in the cold substages of MIS 5 (5d and 5b). These cold periods are highlighted in blue bars.

GL-1248 was more expressive up to 3.21 and 1.27, respectively (**Figure 6**). This suggests that parental rock from the sediments belongs to the felsic rock, or that there is a lack of deep-sourced mafic and ultramafic components (Liu et al., 2015). Thus, the Eu anomaly can be used to study the sources of sedimentary rocks (Taylor and McLennan, 1985; Liu et al., 2015).

As mentioned in the previous topic, the detritic end-members are an effective REE-carrier phase in the sediments of core GL-1248. In the detritic phase carrying REEs, the most common was occurrence was no anomaly unless it is inherited from the continental source (some minerals may have an anomaly). In this work, strong positive Eu anomalies are observed in modern values during the interglacial period, following a sharp decline towards the glacial period registered in the core GL-1248 (**Figure 2**). During the process of partial intracrustal fusion, Eu^{+3} reduces to Eu^{+2} and replaces with Ca^{+2}-bearing minerals, as of feldspar. Hence, the lower crustal has a feldspar-rich, and upper crustal rocks depleted of Eu relative to other REEs. This anomaly is usually propagated into the oceans by weathering and river transported delivery of continental rocks (Abdalla, 2012).

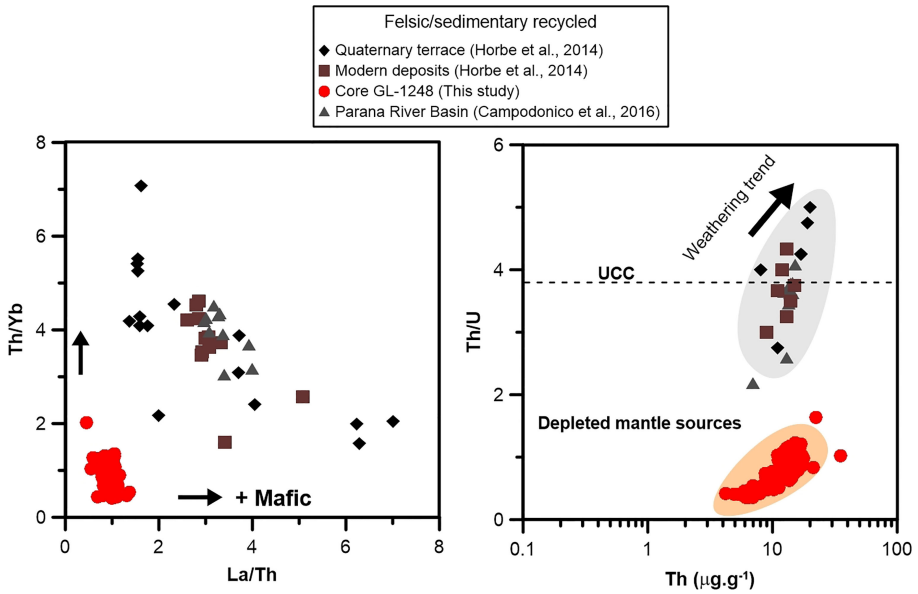

FIGURE 6 | Diagrams of the classification of the sediments by McLennan et al. (1993). Red symbols indicate samples of core GL-1248; Black symbols indicates quaternary terrace samples from the Amazon basin (Horbe et al., 2014); Brown symbols indicates modern deposits samples from the Amazon basin (Horbe et al., 2014); and grey symbols indicate samples of the Parana River basin (Campodonico et al., 2016).

Therefore, positive Eu anomalies are usually a particular factor inherited from specific source rocks since this signal is recorded from the magmatic process until its deposition. The slight positive Eu anomalies were observed in the Amazon basin, where the Amazon River at Óbidos varied between 1.16 and 1.39 (Rousseau et al., 2019), Solimões River varied between 0.98 and 1.36, and Madeira River varied between 1.01 and 1.31 (values calculated by Viers et al. (2008). As well as for fluvial sediment from the Orinoco basin and Maroni Basin that varied between 1.08 and 1.23, and 1.40 and 1.64, respectively (Rousseau et al., 2019). Marine sediments located in Santos Basin (southern Atlantic) had a slightly positive Eu anomaly varied between 0.978 and 1.33 (this study). Picouet et al. (2002) observed strong Eu anomalies in the Niger River (Africa) associated with granitic rocks present in the drainage basin that had this characteristic.

In the igneous systems, positive Eu anomalies found in siliciclastic sediment are also explained by preferential retention by feldspars such as plagioclases and potassium feldspars, particularly in felsic melts (Terekhov and Shcherbakova, 2006; Campodonico et al., 2016). This can be observed in **Figure 6** showing the origin of sediment source according to Taylor and McLennan (1985), which indicates that core GL-1248 derived from a more felsic and/or recycled sedimentary source, as described by others (Absar and Sreenivas, 2015; Liu et al., 2015; Campodonico et al., 2016). In addition, our Sm/Nd data compared with data from the Eu/Eu* (this study) and Sr isotopes (Sousa et al., 2021), illustrated in **Figure 7**, also suggest more felsic end members, as the more differentiated the igneous rock, that is, the more felsic it is, the lower the Sm/Nd ratio will be. It is 0.325 in the chondritic mantle and 0.173 in the PAAS, which represents the upper continental crust. The $^{87}Sr/^{86}Sr$ can be interpreted as the lower, the more basic end member, the higher, and the more felsic. Therefore in this case, when the Sr isotope ratio goes up and Sm/Nd goes down (coinciding peaks in the diagram), they indicate felsic sources entering. This indicates the origin of positive Eu anomalies in marine sediment was from a felsic magma in the Parnaíba basin with assimilation of feldspar during fractionation crystallization over the Last Interglacial.

CONCLUSION

Rare Earth Elements concentration records in core GL-1248 collected from the continental slope off northeastern Brazil had a wide range over the Last Interglacial. The Parnaíba River was the main source of REEs content to the western South Atlantic. Fe elements (Fe-oxyhydroxides) produced *via* weathering of continental and tropical soils were the principal REE-carrier phase in the soils, during transportation until immobilization at core site GL-1248. Regional factors, such as climate, rainfall regime, runoff events, and relative sea-level changes contributed significantly to continental-REEs erosion of sedimentary layers of the Parnaíba Basin, and transport and deposition of mobilized REE from the continent to the study site.

Peaks in REEs were correlated with peaks of Ti/Ca ratios from NE Brazil verifying that REEs content delivered at our site was transported with fluvial materials during continental runoff events corresponding to millennial-scale variability. Furthermore,

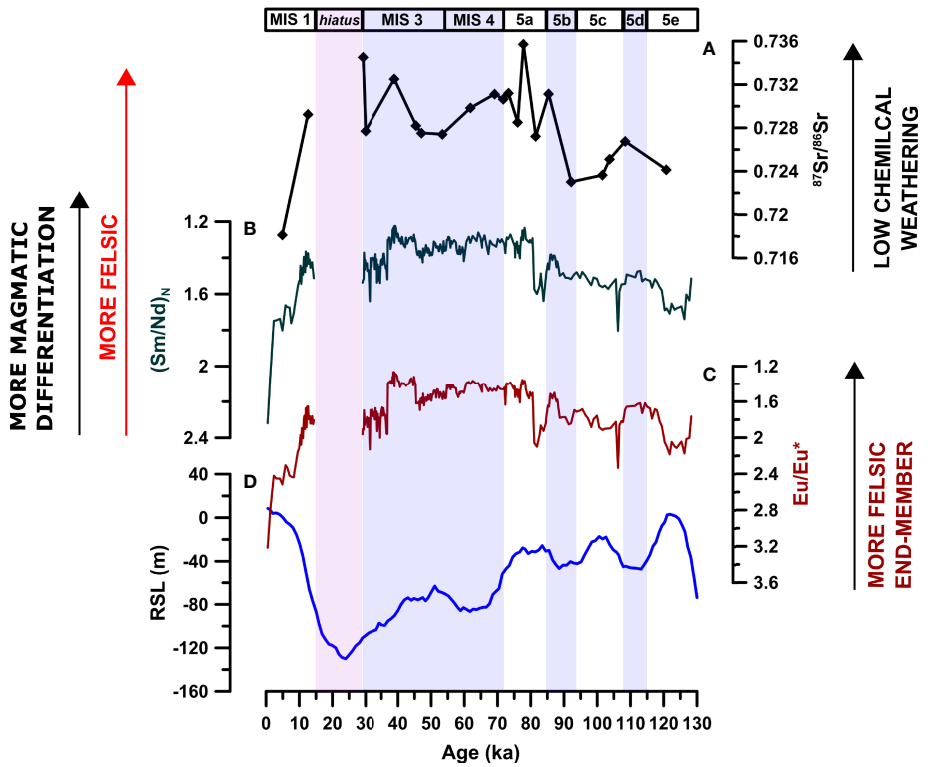

FIGURE 7 | Glacial-Interglacial variability as shown by the comparison diagram between felsic sources in core GL-1248: **(A)** $^{87}Sr/^{86}Sr$ isotopes ratios (Sousa et al., 2021) (black line); **(B)** Sm/Nd ratios normalized by PAAS (this study) (dark green line); **(C)** Eu/Eu* anomalies (this study) (dark red line); and **(D)** Relative sea-level from (Waelbroeck et al., 2002) (blue line). MIS boundaries in the studied time interval are numbered from 1 to 5, except 2 (hiatus), as well as in the cold substages of MIS 5 (5d and 5b). These cold periods are highlighted in blue bars.

variation in sea-level changes and precipitation patterns influence its deposition as well as transportation.

Changes in the negative Ce-anomaly obtained in sediment showed not behave as a proxy for changes in deep ocean oxygenation during the interglacial relative to the last glacial period. Here, we observed that variation was caused by glacial-interglacial variations in sea level through its control over the exposure of the continental shelf. Given its flat morphology, eustatic changes in sea level during glacial-interglacial cycles can result in rapid exposure or drowning of the continental shelf on the Brazilian equatorial margin.

The origin of positive Eu anomalies in siliciclastic sediment was explained by preferential retention by feldspars such as plagioclases and potassium feldspars, particularly in felsic melts. In core GL-1248, this anomaly was caused by a felsic magma from the Parnaíba Basin with assimilation of felspar during fractionation crystallization since the Last Interglacial.

DATA AVAILABILITY STATEMENT

The original contributions presented in the study are included in the article/**Supplementary Material**. Further inquiries can be directed to the corresponding author.

AUTHOR CONTRIBUTIONS

TS: conceptualization and writing - original draft. IV: writing and review and editing. EM: writing and review. TF: writing and review. RN: writing and review. JS: writing and review. AA: review and funding acquisition. CV: supervision, review, editing. ES-F: supervision, conceptualization writing, review editing, and funding acquisition. All authors contributed to the article and approved the submitted version.

FUNDING

This study was financed in part by the Coordenação de Aperfeiçoamento de Pessoal de Nível Superior – Brasil (CAPES) – Finance Code 001. Currently, The Fundação de Amparo a Pesquisa do Estado do Rio de Janeiro – FAPERJ is responsible for funding TS research. CAPES financially supported IV with a scholarship (grant 88887.156152/2017-00). This study was financed in part by CNPq Project RAiN (grant 406322/2018-0).

ACKNOWLEDGMENTS

We appreciate the support of CAPES-ASPECTO project (Grant 88887.091731/2014-01). We thank R. Kowsman (CENPES/

Petrobras) and Petrobras Core Repository staff (Macaé/Petrobras) for providing sediment core GL-1248. This study was financed in part by CNPq Project RAiN (grant 406322/2018-0) and INCT-TMCOcean (INCT-Continent-Ocean Material Transfer – II CNPq, process No. 465.290/2014-0).

SUPPLEMENTARY MATERIAL

The Supplementary Material for this article can be found online at: https://www.frontiersin.org/articles/10.3389/fmars.2022.846976/full#supplementary-material

Supplementary Table 1 | Summary of the total REE concentrations, REE-sum, and their ratio of the marine sediments from the Coast of Northeast Brazil (GL-1248) since the Last Interglacial. MIS is Marine Isotope Stage; LREE is light rare earth elements; HREE is heavy rare earth elements.

Supplementary Table 2 | Distribution of Trace elements, ratios PAAS-normalized (Post-Archean Australian Shale), and occurrence anomalies of the marine sediments from the Coast of Northeast Brazil (GL-1248) since the Last Interglacial. MIS is Marine Isotope Stage.

Supplementary Table 3 | Mineral array in selected samples of marine sediment GL-1248 with corresponding to ages (ka), Marine Oxygen Isotope Stage (MIS), radiogenic isotopes, main mineral source, minerals abundances. Minerals are differentiated into main minerals, other minerals, and trace minerals by red, green, and black text colors, respectively.

REFERENCES

Abdalla, N. R. (2012). *Rare Earth Elements as a Paleo-Ocean Redox Proxy Within the Union Springs Member of the Marcellus Formation. Pennsylvania 2012. 41 F. Thesis (Bachelor of Science) - Department of Geosciences* (Pennsylvania: College of Earth and Mineral Sciences, The Pennsylvania State University).

Absar, N., and Sreenivas, B. (2015). Petrology and Geochemistry of Greywackes of the ~1.6 Ga Middle Aravalli Supergroup, Northwest India: Evidence for Active Margin Processes. *Int. Geol. Rev.* 57 (2), 134–158. doi: 10.1080/00206814.2014.999355

Antonina, N., Shazili, M., Yunus, K., Chuan, O. M., Yaacob, R., and Sharifah, F. N. (2013). Geochemistry of the Rare Earth Elements (Ree) Distribution in Terengganu Coastal Waters: A Study Case From Redang Island Marine Sediment. *Open J. Mar. Sci.* 03, 154–159. doi: 10.4236/ojms.2013.33017

Arz, H. W., Pätzold, J., and Wefer, G. (1998). Correlated Millennial-Scale Changes in Surface Hydrography and Terrigenous Sediment Yield Inferred From Last-Glacial Marine Deposits Off Northeastern Brazil. *Quat. Res.* 50 (2), 157–166. doi: 10.1006/qres.1998.1992

Arz, H. W., Pätzold, J., and Wefer, G. (1999). Climatic Changes During the Last Deglaciation Were Recorded in Sediment Cores From the Northeastern Brazilian Continental Margin. *Geo-Mar. Lett.* 19 (3), 209–218. doi: 10.1007/s003670050111

Bentahila, Y., Othman, D. B., and Luck, J. M. (2008). Strontium, Lead and Zinc Isotopes in Marine Cores as Tracers of Sedimentary Provenance: A Case Study Around Taiwan Orogen. *Chem. Geol.* 248 (1), 62–82. doi: 10.1016/j.chemgeo.2007.10.024

Bigham, J. M., Fitzpatrick, R. W., and Schulze, D. (2002). Soil Mineralogy With Environmental Applications. Madison. *Soil Sci. Soc Am. J.*, 7 323–366. doi: 10.2136/sssabookser7. Iron oxides. In: Dixon, J.B. Schulze, D.G.

Bohm, E., Lippold, J., Gutjahr, M., Frank, M., Blaser, P., Antz, B., et al. (2014). Strong and Deep Atlantic Meridional Overturning Circulation During the Last Glacial Cycle. *Nature.* 517 (7532), 73–76. doi: 10.1038/nature14059

Bouchez, J., Gaillardet, J., France-Lanord, C., Maurice, L., and Dutra-Maia, P. (2011). Grain Size Control of River Suspended Sediment Geochemistry: Clues From Amazon River Depth Profiles. *Geochem. Geophys. Geosyst.* 12 (3), 1–24. doi: 10.1029/2010GC003380

Campodonico, V. A., García, M. G., and Pasquini, A. I. (2016). The Geochemical Signature of Suspended Sediments in the Parana River Basin: Implications for Provenance, Weathering, and Sedimentary Recycling. *Catena.* 143, 201–214. doi: 10.1016/j.catena.2016.04.008

Chalk, T. B., Foster, G. L., and Wilson, P. A. (2019). Dynamic Storage of Glacial CO_2 in the Atlantic Ocean Revealed by Boron [$CO_3$2-] and Ph Records From ODP Hole 162-980A, 162-980B and 162-908C. *Pangaea*. 510, 1–11. doi: 10.1594/PANGAEA.898075

Crusius, J., and Thomson, J. (2000). Comparative Behavior of Authigenic Re, Mo and U During Reoxidation and Subsequent Long-Term Burial in Marine Sediments. *Geochim. Cosmochim. Acta* 64, 2233–2243. doi: 10.1016/S0016-7037(99)00433-0

Cruz, F. W., Burns, S. J., Karmann, I., Sharp, W. D., and Vuille, M. (2006). Reconstruction of Regional Atmospheric Circulation Features During the Late Pleistocene in Subtropical Brazil From Oxygen Isotope Composition of Speleothems. *Earth Planet. Sci. Lett.* 248 (1–2), 494–506. doi: 10.1016/j.epsl.2006.06.019

Curry, W. B., and Oppo, D. W. (2005). Glacial Water Mass Geometry and the Distribution of δ 13C of ΣCO_2 in the Western Atlantic Ocean. *Paleoceanography.* 20 (1), 1–12. doi: 10.1029/2004PA001021

De Baar, H. J. W., Bacon, M. P., and Brewer, P. G. (1983). Rare-Earth Distributions With a Positive Ce Anomaly in the Western North Atlantic Ocean. *Nature.* 301 (5898), 324–327. doi: 10.1038/301324a0

Depetris, P. J., Probst, J.-L., Pasquini, A. I., and Gaiero, D. M. (2003). The Geochemical Characteristics of the Paraná River Suspended Sediment Load: An Initial Assessment. *Hydrol. Process.* 17 (7), 1267–77. doi: 10.1002/hyp.1283

De Sousa, T. A., Venancio, I. M., Valeriano, C. M., Heilbron, M., Dias Carneiro Weitzel,M. T., Mane, M. A., et al (2021). Changes in Sedimentary Provenance and Climate Off the Coast of Northeast Brazil Since the Last Interglacial. *Mar. Geol.* 435, 106454. doi: 10.1016/j.margeo.2021.10

Dupont, L. M., Schlütz, F., Ewah, C. T., Jennerjahn, T. C., Paul, A., and Behling, H. (2010). Two-Step Vegetation Response to Enhanced Precipitation in Northeast Brazil During Heinrich Event 1. *Glob. Chang. Biol.* 16, 1647–60. doi: 10.1111/j.1365-2486.2009.02023.x

Elderfield, H., and Pagett, R. (1986). Rare Earth Elements in Ichthyolites: Variations With Redox Conditions and Depositional Environment. *Sci. Total Environ.* 49, 175–197. doi: 10.1016/0048-9697(86)90239-1

Fadina, O. A., Venancio, I. M., Belem, A., Silveira, C. S., de Castro Bertagnolli, ,. D., Silva-Filho, E. V., et al. (2019). Paleoclimatic Controls on Mercury Deposition in Northeast Brazil Since the Last Interglacial. *Quat. Sci. Rev.* 221, 105869. doi: 10.1016/j.quascirev.2019.105869

German, C. R., and Elderfield, H. (1990). Application of the Ce Anomaly as a Paleoredox Indicator: The Ground Rules. *Paleoceanography* 5 (5), 823–833. doi: 10.1029/PA005i005p00823

Gottschalk, S., Fehm, T. F., Deán-Ben, X. L., Tsytsarev, V., and Razansky, D. (2016). Correlation Between Volumetric Oxygenation Responses and Electrophysiology Identifies Deep Thalamocortical Activity During Epileptic Seizures. *Neurophotonics* 4 (1), 011007. doi: 10.1117/1.nph.4.1.011007

Govin, A., Holzwarth, U., Heslop, D., Ford Keeling, L., Zabel, M., Mulitza, S., et al. (2012). Distribution of Major Elements in Atlantic Surface Sediments (36°N-49°s): Imprint of Terrigenous Input and Continental Weathering. *Geochem. Geophys. Geosyst.* 13 (1), 1–23. doi: 10.1029/2011GC003785

Henderson, P. (1984). *Rare Earth Elements Geochemistry* (Amsterdam -Oxford -New York -Tokyo: Elsevier), 1984.

Hodgson, D. A., Verleyen, E., Squier, A. H., Sabbe, K., Keely, B. J., Saunders, K. M., et al. (2006). Interglacial Environments of Coastal East Antarctica: Comparison of MIS 1 (Holocene) and MIS 5e (Last Interglacial) Lake-Sediment Records. *Quat. Sci. Rev.* 25 (1-2), 179–197. doi: 10.1016/j.quascirev.2005.03.004

Hoogakker, B. A. A., Elderfield, H., Schmiedl, G., McCave, I. N., Rickaby, R. E. M., and Shackleton, N. J. (2015). Bottom Water Oxygen Reconstructions Iberian Margin Sediment Core MD95-2042 Between 0 and 150,000 Years BP. *Pangaea* 8 (1), 40–3. doi: 10.1594/PANGAEA.856564

Horbe, A. M.C., da Trindade, I. R., Dantas, E. L., Santos, R. V., and Roddaz, M. (2014). Provenance of Quaternary and Modern Alluvial Deposits of the Amazonian Floodplain (Brazil) Inferred From Major and Trace Elements

and Pb–Nd–Sr Isotopes. *Palaeogeogr. Palaeoclimatol. Palaeoecol.*, 411, 144–54. doi: 10.1016/j.palaeo.2014.06.019

Jaccard, S., and Galbraith, E. (2012). Large Climate-Driven Changes of Oceanic Oxygen Concentrations During the Last Deglaciation. *Nat. Geosci.* 5, 151–156. doi: 10.1038/NGEO1352

Jaccard, S., Galbraith, E., Martínez-García, A., and Anderson, R. (2016). Covariation of Deep Southern Ocean Oxygenation and Atmospheric CO_2 Through the Last Ice Age. *Nature.* 530, 207–210. doi: 10.1038/nature16514

Jaeschke, A., Rühlemann, C., Arz, H., Heil, G., and Lohmann, G. (2007). Coupling of Millennial-Scale Changes in Sea Surface Temperature and Precipitation Off Northeastern Brazil With High-Latitude Climate Shifts During the Last Glacial Period. *Paleoceanography* 22 (4), 1–10. doi: 10.1029/2006PA001391

Johnsson, M. J., Stallard, R.F., and Lundberg, N. (1991). Controls on the Composition of Fluvial Sands From a Tropical Weathering Environment: Sands of the Orinoco Drainage Basin, Venezuela and Colombia. *Bull. Geol. Soc. Am.*, 103:1622–647.

Johnsson, M. J. (1993). The System Controlling the Composition of Clastic Sediments. *Geol. Soc. Am. Spec. Pap.*, 1–20. doi: 10.1130/spe284-p1

Lisiecki, L. E., and Raymo, M. E. (2005). A Pliocene-Pleistocene Stack of 57 Globally Distributed Benthic δ^{18}o Records. *Paleoceanography* 20 (1). doi: 10.1029/2004pa001071

Liu, Y., Cheng, Y., Liu, J., Zhang, L., Zhang, C., and Zheng, C. (2015). Provenance Discrimination of Surface Sediments Using Rare Earth Elements in the Yalu River Estuary, China. *Environ. Earth Sci.* 74 (4), 3507–3517. doi: 10.1007/s12665-015-4391-x

Liu, Y.-G., Miah, M. R. U., and Schmitt, R. A. (1988). Cerium: A Chemical Tracer for Paleo-Oceanic Redox Conditions. *Geochim. Cosmochim. Acta* 52 (6), 1361–1371. doi: 10.1016/0016-7037(88)90207-4

Liu, Y.-G., and Schmitt, R. A. (1990). Elemental Abundances in Marine Carbonates From ODP Leg 115 Holes (Table 1). *Pangaea* 115, 709–14,. doi: 10.1594/PANGAEA.755473

Liu, Y. G., and Schmitt, R. A. (1990). "Cerium Anomalies in Western Indian Ocean Cenozoic Carbonates, Leg 115," in *Proc. of the Ocean Drilling Program. Scientific Results*, vol. Vol. I IS . Ed. R. A. Duncan (TX, USA: Ocean Drilling Program, College Station), 709–7 14, pp.

Cerium Anomalies in WesternMartrat, B., Jimenez-Amat, P., Zahn, R., and Grimalt, J. O. (2014). Similarities and Dissimilarities Between the Last Two Deglaciations and Interglaciations in the North Atlantic Region. *Quat. Sci. Rev.* 99, 122–134. doi: 10.1016/j.quascirev.2014.06.016

McLennan, S. M., Hemming, S., McDaniel, D. K., and Hanson, G. N. (1993). Geochemical Approaches to Sedimentation, Provenance, and Tectonics. *Geol. Soc. Am. Spec. Pap.* 284, 21–40. doi: 10.1130/spe284-p21

Milliman, J. M., and Meade, R. H. (1983). Worldwide Delivery of River Sediment to the Oceans. *J Geol.*, 91, 1–21.

Members, N. (2004). High-Resolution Record of Northern Hemisphere Climate Extending Into the Last Interglacial Period. *Nature.* 431 (7005), 147–151. doi: 10.1038/nature02805

Morton, A. C., and Hallsworth, C. R. (1999). Processes Controlling the Composition of Detrital Heavy Mineral Assemblages in Sandstones. *Sedimentary Geology* 124, 3–29. doi: 10.1016/S0037-0738(98)00118-3

Murray, R. W., Brink, M. R. B., Brumsack, H. J, Gerlach, D. C., and Russ, G. P.III (1991). Rare Earth Elements in Japan Sea Sediments and Diagenetic Behavior of Ce/Ce∗: Results From ODP Leg 127. *Geochim. Cosmochim. Acta* 55 (9), 2453–2466. doi: 10.1016/0016-7037(91)90365-C

Murray, R. W., Buchholtz Ten Brink, M. R., Jones, D. L., Gerlach, D. C., and Russ, G. P. III. (1990a). Rare Earth Elements as Indicators of Different Marine Depositional Environments in Chert and Shale. *Geology* 18 (3), 268. doi: 10.1130/0091-7613(1990)018<0268:reeaio>2.3.co;2

Nace, T. E., Baker, P. A., Dwyer, G. S., Silva, C. G., Rigsby, C. A., Burns, S. J., et al. (2014). The Role of North Brazil Current Transport in the Paleoclimate of the Brazilian Nordeste Margin and Paleoceanography of the Western Tropical Atlantic During the Late Quaternary. *Paleogeogr. Palaeoclimatol. Palaeoecol.* 415, 3–13. doi: 10.1016/j.palaeo.2014.05.030

Pattan, J. N., Pearce, N. J. G., and Mislankar, P. G. (2005). Constraints in Using Cerium-anomaly of Bulk Sediments as an Indicator of Paleo Bottom Water Redox Environment: A Case Study From the Central Indian Ocean Basin. *Chem. Geol.* 221 (3–4), 260–278. doi: 10.1016/j.chemgeo.2005.06.009

Picouet, C., Dupré, B., Orange, D., and Valladon, M. (2002). Major and Trace Element Geochemistry in the Upper Niger River (Mali): Physical and Chemical Weathering Rates and CO_2 Consumption. *Chem. Geol.* 185 (1-2), 93–124. doi: 10.1016/s0009-2541(01)00398-9

Piacsek, P., Behling, H., Gu, F., Venancio, I., Lessa, D., Belem, A., et al (2021). Changes in Sea Surface Hydrography and Productivity in the Western Equatorial Atlantic Since the Last Interglacial *Palaeogeogr. Palaeoclimatol. Palaeoecol.* 562. 10.1016/j.palaeo.2020.109952.

Pourmand, A., Dauphas, N., and Ireland, T. J. (2012). A Novel Extraction Chromatography and MC-ICP-MS Technique for Rapid Analysis of REE, Sc, and Y: Revising CI-chondrite and Post-Archean Australian Shale (PAAS) Abundances. *Chem. Geol.* 291, 38–54. doi: 10.1016/j.chemgeo.2011.08.011

Rahmstorf, S. (2002). Ocean Circulation and Climate During the Past 120,000 Years. *Nature.* 419, 207–214. doi: 10.1038/nature01090

Rama-Corredor, O., Martrat, B., Grimalt, J. O., Lopez Otalvaro, G. E., Flores, J. A., and Sierro, F. (2015). Parallelisms Between Sea Surface Temperature Changes in the Western Tropical Atlantic (Guiana Basin) and High Latitude Climate Signals Over the Last 140 000 Years. *Clim. Past.* 11, 1297–1311. doi: 10.5194/cp-11-1297-2015

Revel, M., Ducassou, E., Grousset, F. E., Bernasconi, S. M., Migeon, S., Revillon, S., et al (2010). 100,000 Years of African Monsoon Variability Recorded in Sediments of the Nile Margin *Quat. Sci. Rev.* 29 (11), 1342–1362. doi: 10.1016/j.quascirev.2010.02.006

Revel, M., Colin, C., Bernasconi, S., Combourieu-Nebout, N., Ducassou, E., Grousset, F.E., et al (2014). 21,000 Years of Ethiopian African Monsoon Variability Recorded in Sediments of the Western Nile Deep-Sea Fan. *Reg. Environ. Change* 14 (5), 1685–1696. doi: 10.1007/s10113-014-0588-x

Revel, M., Ducassou, E., Skonieczny, C., Colin, C., Bastian, L., Bosch, D., et al (2015). 20,000 Years of Nile River Dynamics and Environmental Changes in the Nile Catchment Area as Inferred From Nile Upper Continental Slope Sediments *Quat. Sci. Rev.* 130, 200–221. doi: 10.1016/j.quascirev.2015.10.030

Rohling, E. J., Grant, K., Hemleben, C., Siddall, M., Hoogakker, B. A. A., Bolshaw, M., et al. (2007). High Rates of Sea-Level Rise During the Last Interglacial Period. *Nat. Geosci.* 1 (1), 38–42. doi: 10.1038/ngeo.2007.28

Rousseau, T. C. C., Roddaz, M., Moquet, J. S., Handt Delgado, H., Calves, G., and Bayon, G. (2019). Controls on the Geochemistry of Suspended Sediments From Large Tropical South American Rivers (Amazon, Orinoco, and Maroni). *Chem. Geol.* 522, 38–54. doi: 10.1016/j.chemgeo.2019.05.027

Rühlemann, C., Frank, M., Hale, W., Mangini, A., Mulitza, S., Müller, P. J., et al. (1996). Late Quaternary Productivity Changes in the Western Equatorial Atlantic: Evidence From ^{230}Th-Normalized Carbonate and Organic Carbon Accumulation Rates. *Mar. Geol.* 135 (1–4), 127–152. doi: 10.1016/S0025-3227(96)00048-5

Schijf, J., de Baar, H. J. W., and Millero, F. J. (1994). Kinetics of Ce and Nd Scavenging in Black Sea Waters. *Mar. Chem.* 46 (4), 345–359. doi: 10.1016/0304-4203(94)90031-0

Seaman, J. C. (2013). Competitive Sorption and Transport of Heavy Metals in Soils and Geological Media. *Soil Sci. Soc Am. J.* 77 (6), 2216. doi: 10.2136/sssaj2013.0004br

Taylor, S. R., and McLennan, S. M. (1985). The Continental Crust: Its Composition and Evolution. *Phys. Earth Planet. Inter.* 42 (3), 196–197. doi: 10.1016/0031-9201(86)90093-2

Terekhov, E. N., and Shcherbakova, T. F. (2006). Genesis of Positive Eu Anomalies in Acid Rocks From the Eastern Baltic Shield. *Geochem. Int.* 44, 439–455. doi: 10.1134/S0016702906050028

Tostevin, R., Shields, G. A., Tarbuck, G. M., He, T., Clarkson, M. O., and Wood, R. A. (2016). Effective Use of Cerium Anomalies as a Redox Proxy in Carbonate-Dominated Marine Settings. *Chem. Geol.* 438, 146–162. doi: 10.1016/j.chemgeo.2016.06.027

Tribovillard, N., Algeo, T. J., Lyons, T., and Riboulleau, A. (2006). Trace Metals as Paleoredox and Paleoproductivity Proxies: An Update. *Chem. Geol.* 232 (1–2), 12–32,0009-2541. doi: 10.1016/j.chemgeo.2006.02.012

Venancio, I. M., Mulitza, S., Govin, A., Santos, T. P., Lessa, D. O., Albuquerque, A., et al. (2018). Millennial-to Orbital-Scale Responses of Western Equatorial Atlantic Thermocline Depth to Changes in the Trade Wind System Since the

Last Interglacial. *Paleoceanogr. Paleoclimatol.* 33 (12), 1490–1507. doi: 10.1029/2018PA003437

Viers, J., Roddaz, M., Filizola, N., Guyot, J.-L., Sondag, F., Brunet, P., et al. (2008). Seasonal and Provenance Controls on Nd–Sr Isotopic Compositions of Amazon Rivers Suspended Sediments and Implications for Nd and Sr Fluxes Exported to the Atlantic Ocean. *Earth Planet. Sci. Lett.* 274 (3-4), 511–523. doi: 10.1016/j.epsl.2008.08.011

Waelbroeck, C., Labeyrie, L., Michel, E., Duplessy, J. C., Mcmanus, J. F., Lambeck, K., et al. (2002). Sea-level and Deep-Water Temperature Changes Derived From Benthic Foraminifera Isotopic Records. *Quat. Sci. Rev.* 21 (1-3), 295–305. doi: 10.1016/s0277-3791(01)00101-9

Walter, H.J., Hegner, E., Diekmann, B., and Kuhn, G. (2000). Provenance and Transport of Terrigenous Sediment in the South Atlantic Ocean and Their Relations to Glacial and Interglacial Cycles: Nd and Sr Isotopic Evidence. *Geochim, Cosmochim Acta.* 64 (22), 3813–3827. doi: 10.1016/S0016-7037(00)00476-2

Wang, X., Auler, A. S., Edwards, R. L., Cheng, H., Cristalli, P. S., Smart, P. L., et al. (2004). Wet Periods in Northeastern Brazil Over the Past 210 Kyr Linked to Distant Climate Anomalies. *Nature.* 432, 740. doi: 10.1038/nature03067

Wang, Y.-L., Liu, Y.-G., and Schmitt, R. A. (1986). Rare Earth Element Geochemistry of South Atlantic Deep-Sea Sediments: Ce Anomaly Change at ~54 My. *Geochim. Cosmochim. Acta* 50 (7), 1337–1355. doi: 10.1016/0016-7037(86)90310-8

Wilde, P., Quinby-Hunt, M. S., and Erdtmann, B.-D. (1996). The Whole-Rock Cerium Anomaly: A Potential Indicator of Eustatic Sea-Level Changes in Shales of the Anoxic Facies. *Sediment. Geol.* 101 (1-2), 43–53. doi: 10.1016/0037-0738(95)00020-8

Wolff, E. W., Chappellaz, J., Blunier, T., Rasmussen, S. O., and Svensson, A. (2010). Millennial-scale Variability During the Last Glacial: The Ice Core Record. *Quat. Sci. Rev.* 29 (21–22), 2828–2838. doi: 10.1016/j.quascirev.2009.10.013

Wright-Clark, J., and Holser, W. T. (1981). Rare-Earth Elements in Conodont Apatite as a Measure of Redox Conditions in Ancient Seas. *Geol. Soc Am.* 13, 586.

Xu, F., Li, A., Li, T., Xu, K., Chen, S., Qiu, L., et al. (2011). Rare Earth Element Geochemistry in the Inner Shelf of the East China Sea and Its Implication to Sediment Provenances. *J. Rare. Earths.* 29 (7), 702–709. doi: 10.1016/s1002-0721(10)60526-1

Yusof, A. M., Akyil, S., and Wood, A. K. H. (2001). Rare Earth Elements Determination and Distribution Patterns in Sediments of a Polluted Marine Environment by Instrumental Neutron Activation Analysis. *J. Radioanal. Nucl. Chem.* 249 (2), 333–341. doi: 10.1023/a:1013297932536

Zhang, Y., Chiessi, C. M., Mulitza, S., Zabel, M., Trindade, R. I. F., Hollanda, M. H., et al. (2015). Origin of Increased Terrigenous Supply to the NE South American Continental Margin During Heinrich Stadial 1 and the Younger Dryas. *Earth Planet. Sci. Lett.* 432, 493–500. doi: 10.1016/j.epsl.2015.09.054

Conflict of Interest: The authors declare that the research was conducted in the absence of any commercial or financial relationships that could be construed as a potential conflict of interest.

Publisher's Note: All claims expressed in this article are solely those of the authors and do not necessarily represent those of their affiliated organizations, or those of the publisher, the editors and the reviewers. Any product that may be evaluated in this article, or claim that may be made by its manufacturer, is not guaranteed or endorsed by the publisher.